# 3D Analysis of Fatigue Fracture Morphology Generated by Combined Bending - Torsion

Karel Slámečka and Jaroslav Pokluda
Brno University of Technology, Faculty of Mechanical Engineering, Institute of Physical Engineering, Technická 2896/2, 616 69 Brno, Czech Republic
slamecka@fyzika.fme.vutbr.cz, pokluda@ufi.fme.vutbr.cz

## Abstract

The paper deals with quantitative analysis of morphology of the fracture surfaces generated under pure torsion, pure bending, and mixed bending-torsion loading. Characteristics of roughness and fractality are studied in dependence on loading conditions, profile orientation and distance from the specimen surface, respectively. Moreover, the mismatch between matching profiles is analysed for all investigated specimens. As expected, the surface roughness increases with increasing distance from the specimen surface. A strong increase in the mismatch with increasing torsion component can be considered to be the most important result of the analysis.

## Introduction

A combined bending-torsion is often used when simulating the fatigue exploitation of rotational structural components. Since the fracture surface can be considered to be a degradation process gauge originating from interaction of propagating crack with the material and the environment, fractography became important inherent part of failure analysis, see e.g. Vasilev [1]. On the present, much effort is focused on estimation of local fracture process parameters from the fracture surface morphology or fracture surface images. For example, the stress intensity range $\Delta K$ and overload magnitude were studied using Fourier analyses by Kobayashi [2], the fatigue crack propagation mode was deduced from roughness parameters by Antunes et al. [3] and the crack growth rate was investigated by means of the textural fractography by Lauschmann and Nedbal [4].

A direct study of fracture images is confined to the projection of three-dimensional elements of fracture surface to the projection plane. In this case, the spatial information can be deduced only in a limited range and practically no conclusion can be made on the 3D character of fracture. However, for complex analyses of material fatigue behaviour some spatial characteristics are necessary (in particular the true surface area) and therefore it is desirable to perform 3D analysis. The first part of this task can be solved by a method known as stereofotogrammetry that is briefly discussed bellow. Because there are many approaches to describe surface roughness resulting generally in many descriptive parameters (e.g. Dooley and Bernasek [5], Gadelmawla et al. [6]), the second part of this task is quite more complicated.

## Stereophotogrammetry

Stereophotogrammetry is based on software evaluation of two digitalized images of fracture surface taken from different positions of view (so-called stereopair). Stereoimages are mostly acquired using the scanning electron microscopy providing excellent accuracy

at arbitrary magnification and the high depth of focus making it possible to analyse very rough surfaces such as usually can be encountered in fatigue. Furthermore, the possibility to find corresponding regions on both fracture surfaces rather easily is important for many applications as shown by Kolednik et al. [7]. Stereopair is processed via hierarchical area-based matching algorithm in order to find corresponding (homologue) points on both images. Subsequently, relative *z*-coordinates of all found homologue points are calculated from their shift and known scanning geometry. The output of the procedure is 3D model of depicted surface area consisting of 20,000 – 30,000 points in the case of 1024×768 pixels stereoimages, so-called DEM (digital elevation model). The images with a resolution of up to 4000x3200 pixels can be taken in new SEMs. For such pictures, the number of homologue points may increase by a factor 10 or more. The relative height accuracy better then 3% was estimated by comparison of results obtained by stereophotogrammetry, a profilometry, a confocal microscopy, and an atomic force microscopy (Scherer and Kolednik [8]). For more detail about stereophotogrammetry, see, for example [7,8].

## Measured parameters

### *Profile and surface roughness parameters*

Historically, first compiled quantitative parameters describing surface roughness were all based on amplitude attributes [5], such as the various moments of the height distribution (e.g. skewness *Sk*, kurtosis *K*) or the extreme height value parameters (e.g. lowest point on the surface $R_v$ etc.). In quantitative fractography, the linear (profile) roughness $R_L$ and the surface roughness $R_S$ are commonly used, see e.g. Underwood and Banerji [9]. The linear roughness is a dimensionless quantity determined as the fraction of the true profile length $L$ over its projected length $L´$ onto the macroscopic crack plane:

$$R_L = \frac{L}{L´} \ . \tag{1}$$

The linear roughness $R_L$ take the same values for profiles of the same shape. Analogously, the area roughness $R_S$ is a dimensionless quantity defined as the quotient of the true surface area $S$ and the projected area $S´$:

$$R_S = \frac{S}{S´} . \tag{2}$$

Due to the technical difficulties and the time-consuming analysis, the direct determination of the true surface area is rather sparse. More frequently, this quantity is calculated through some parametric relationships connecting the linear roughness $R_L$ and the surface roughness $R_S$ provided that the specimen is sampled with randomly placed and randomly oriented profile sections perpendicular to the mean fracture surface. As the most prominent, the following linear relationship was proposed [9]:

$$R_S = \left(\frac{4}{\pi}\right)\left(R_L - 1\right) + 1 . \tag{3}$$

Note that for profile consisting of randomly oriented segments $R_L = \pi/2$ and for surface consisting of randomly oriented elements $R_S = 2$.

### *Profile and surface fractal dimension*

In order to interpret correctly roughness parameters discussed in the previous subsection, the fractal character of the fracture surface should be taken into account. The peculiar interaction of all measured fracture lengths with used measuring unit has been many times proven and the idea, that fracture surface can be treated as a fractal, is now well accepted [5, 7-9]. The basic property of fractal object is self-similarity or self-affinity, which causes that when the object is magnified similar finer structure appears. This property is quantified by a constant referred to as a fractal dimension taking values between object's Euclidean dimension and Euclidean dimension of space in which object is embedded.

Fractal behaviour of irregular fracture profile is illustrated in Fig. 1, where the increasing measured apparent length $L$ with decreasing measuring unit $\lambda$ can be observed. This dependence is described by theoretical fractal equation:

$$L(\lambda) = L_0 \lambda^{-(D_L - 1)}, \tag{4}$$

where $L_0$ is a constant with the dimension of length, and $D_L$ is the fractal dimension of the profile.

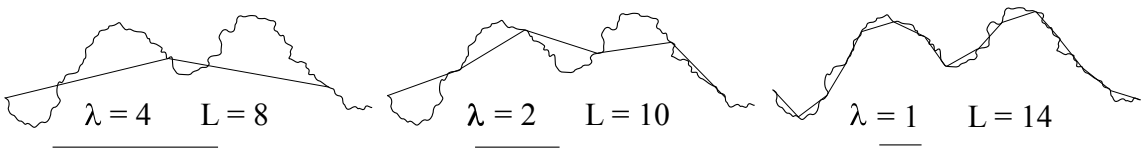


FIGURE 1. Dependence of irregular profile's apparent length $L$ on used measuring unit λ.

Equation (4) can be modified in order to obtain relation to the profile roughness parameter:

$$R_L(\lambda) = C_1 \lambda^{-(D_L - 1)}, \tag{5}$$

where $C_1$ is a dimensionless constant. Similarly, the relation between surface roughness $R_S$ and the fractal dimension $D_S$ is given as

$$R_S\left(\lambda^2\right) = C_2\left(\lambda^2\right)^{-(D_S - 2)/2} = C_2 \lambda^{-(D_S - 2)}, \tag{6}$$

where $\lambda^2$ is the area measurement unit and $C_2$ is a dimensionless constant.

In fact, natural fracture surfaces and fracture profiles rarely exhibit behaviour predicted by equation (4). Instead of linear dependency, there is a trend toward a sigmoidal curvature in *log* $\lambda$ - *log* $L$ coordinates, as shown by Underwood and Banerji [10]. However, since the equation (4) is for the most cases respected in sufficiently wide range of $\lambda$ (for herein calculated profiles from 1μm up to 30μm), the fractal dimension extracted from this part of chart is a commonly used parameter [7,8].

## Experimental

### *Material and specimen loading*

The symmetric in-phase sinusoidal bending-torsion loading was applied to smooth cylindrical specimens made of high-strength low alloy steel using the fatigue machine MZGS-100 of the Polish provenience. The heat treatment and tensile mechanical

properties of the material are displayed in Tab.1. Loading conditions and the experimental fatigue life data are shown in Tab.2, where $\sigma_a$ is the amplitude of maximal bending stress, $\tau_a$ is the amplitude of maximal torsion stress, $\eta$ is the loading parameter and $N_f$ is the number of cycles to failure. The fatigue life of all investigated specimens lies within the boundary region between high- and low-cycle fatigue ($N_f \in (10^4, 10^5)$).

TABLE 1. Heat treatment and tensile mechanical properties

| Heat treatment | Annealing | Quenching | Tempering |
|---|---|---|---|
| | 920 °C/ 25 min. air | 930°C/ 25 min. oil | 650°C/ 40 min. air |

| Mechanical properties | Yield stress / MPa | Ultimate stress / MPa | Elongation / % | Contraction / % |
|---|---|---|---|---|
| | 834 – 844 | 934 - 966 | 13,8 – 14,5 | 49,2 – 52,1 |

TABLE 2. Experimental data

| | $\sigma_a$ / MPa | $\tau_a$ / MPa | $\eta=\tau_a/(\sigma_a+\tau_a)$ | $N_f$ / cycles |
|---|---|---|---|---|
| Pure bending | 738 | 0 | 0 | 102560 |
| Combined bending - torsion | 559,86 | 203,38 | 0,266 | 14880 |
| | 329,37 | 330,30 | 0,501 | 68400 |
| | 135,95 | 372,82 | 0,733 | 100160 |
| Pure torsion | 0 | 399 | 1 | 100400 |

***Stereofotogrammetrical surface topography measurement***

Stereoimages of regions in various distances from specimen surface were taken using the scanning electron microscope LEO S440 by tilting the specimen by an angle 7º-10º in dependence on surface topography complexity. The stereophotogrammetrical reconstructions were performed via commercial software system MEX. Triangulation of all points of the DEM enabled us to extract profiles from corresponding regions on both specimen halves near the fatigue crack initiation as well as to calculate surface roughness $R_S$. Determination of surface fractal dimension $D_S$ can be made by consideration of DEMs containing various numbers of points**.** The mismatches between matching profiles and profile characteristics $R_L$ and $D_L$ were calculated using software application developed in Borland Delphi 7.

## Results and discussion

The linear roughness $R_L$ and the profile fractal dimension $D_L$ in dependence on the profile orientation (with respect to the referential radial direction) are plotted in Fig. 2. Full and empty symbols correspond to profile values obtained from first or second fracture surfaces, respectively. In order to preserve the lucidity, regression curves are plotted only for second fracture surface represented by empty symbols. The centre of the investigated area was at the distance of $0.12R$ from the specimen surface ($R$ is the radius of the specimen cross-section). Fracture surface roughness $R_S$ and surface fractal dimension $D_S$ as a function of the distance from the specimen surface are plotted in Fig. 3. In all figures the regression curves for particular specimens are inscribed with loading parameter $\eta$.

Except for the specimen $\eta$=0,73, the linear roughness $R_L$ tends to increase with increasing deflection from the referential direction whereas profile fractal dimension $D_L$ remains practically constant. Both measured linear parameters seem to be independent on loading conditions and they reach the highest values for the specimen of $\eta$=0,50. As expected, the surface quantities $R_S$ and $D_S$ significantly depend on the distance from the specimen surface due to the increasing plastic deformation ahead the growing crack front.

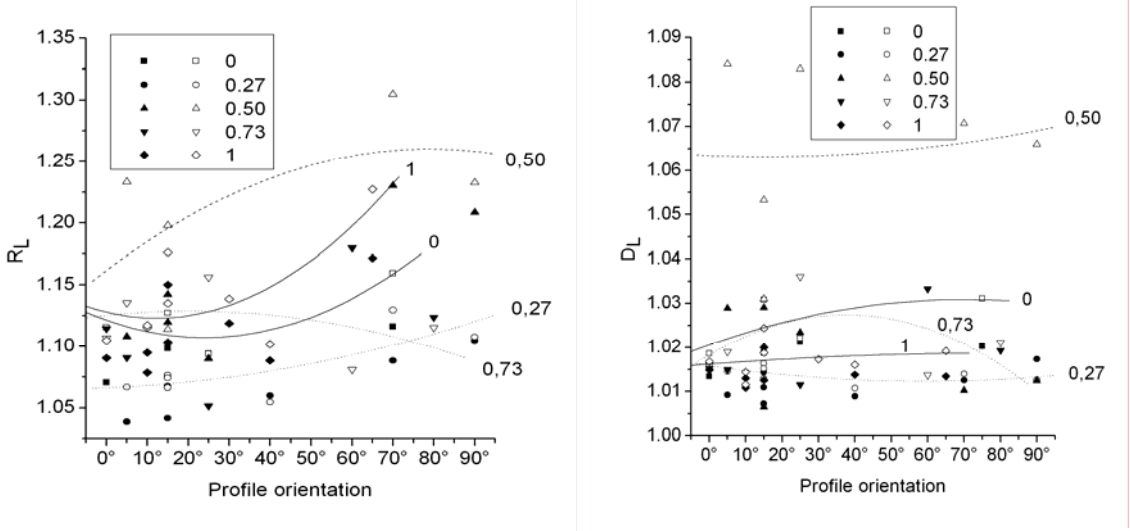


FIGURE 2. The linear roughness $R_L$ and the profile fractal dimension $D_L$ in dependence on profile orientation with respect to the referential radial direction.

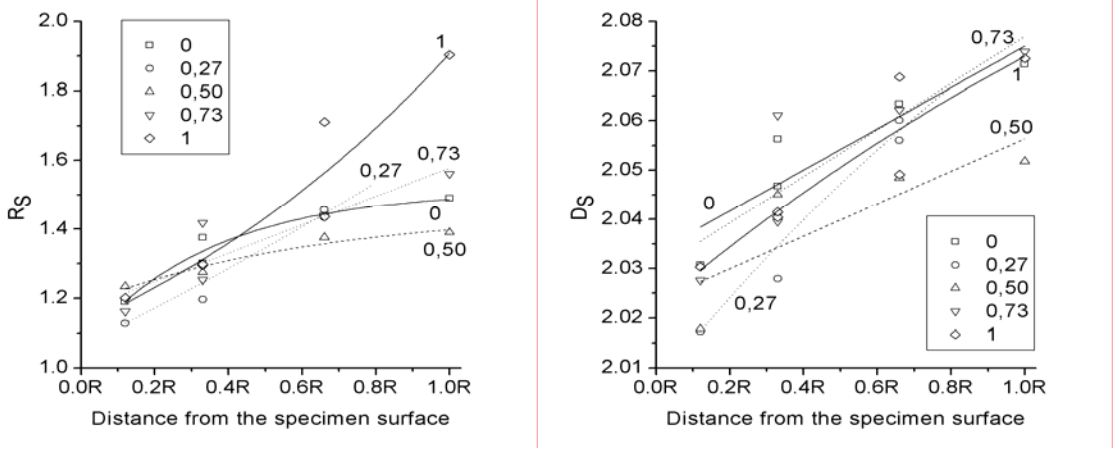


FIGURE 3. Fracture surface roughness $R_S$ and surface fractal dimension $D_S$ as a function of the distance from the specimen surface ($R$ is the specimen radius).

The mismatch between matching profiles from both fracture surfaces in the direction of the crack propagation is depicted in Fig. 4. It is obvious that the torsion component raises misfits between corresponding profiles. This fact may be attributed to an increasing friction contact between fracture surface asperities of sharp edges and high angel facets resulting in abrasion of microparticles leaving empty spaces between corresponding profiles (Pook [11]).

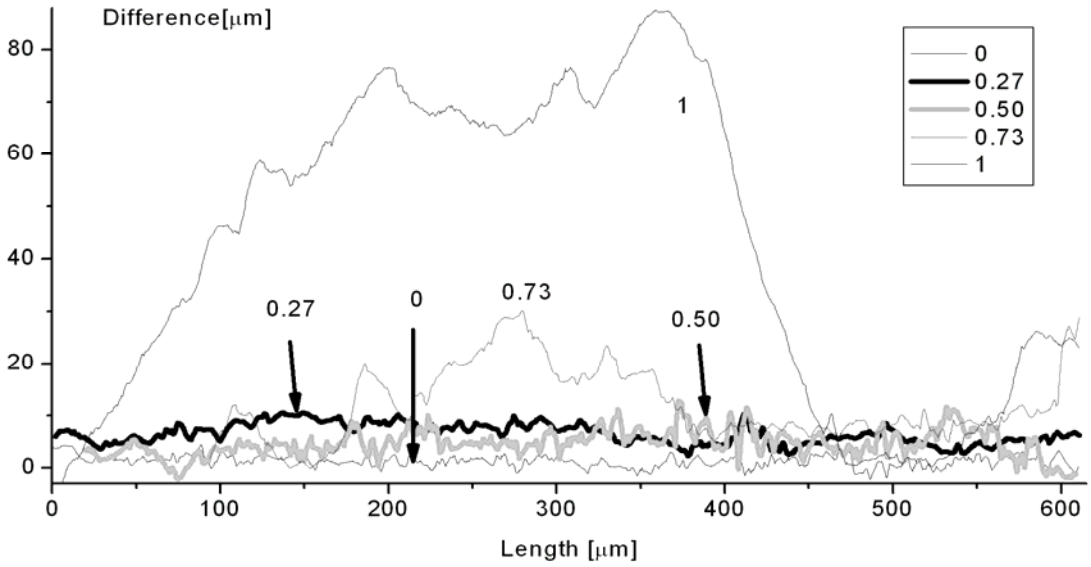


FIGURE 4. The mismatch between matching profiles of both fracture surfaces in the direction of the crack propagation.

## Conclusion

The most convincing results of the 3D-fractography analysis can be summarised into the following points:

- The fractal dimension is unaffected by the proportion of bending/torsion loading.
- The surface roughness increases with increasing distance from the specimen surface.
- The mismatch between matching profiles of fracture surfaces increases with increasing torsion/bending ratio.

## References


1. Vasilev, A.D., *Europ. Microsc. and Analysis*, July 1998, 9-11, 1998.
2. Kobayashi, T., *Int. J. Fatigue*, vol. **19**, 237-244, 1997.
3. Antunes, F.V., Ramalho, A. and Ferreira, J.M., *Int. J. Fatigue*, vol. **22**, 781-788, 2000.
4. Lauschmann, H. and Nedbal, I., *Image Anal Stereol*., vol. **21**, 139-144, 2002.
5. Dooley, P. and Bernasek, S.L., *Surf. Science*, vol. **406,** 206-220, 1998.
6. Gadelmawla, E.S., Koura, M.M., Maksoud, T.M.A., Elewa, I.M. and Soliman, H.H., *J. Mat. Proc. Technol.* **123**, 133-145, 2002.
7. Kolednik, O., Scherer, S., Schwarzböck, P. and Werth, P., In *Fracture mechanics: Applications and Challanges, Proceedings of ECF13,* edited by M. Fuentes and M. Elices, Elsevier, Amsterodam, paper 1U.60, 2000.
8. Scherer, S. and Kolednik, O., *Europ. Microsc. and Analysis*, March 2001, 15-17, 2001.
9. Underwood, E.E. and Banerjee, K., In: *Metals Handbook*, Vol. 12. ASM International, Metals Park, Ohio, USA, 193-210, 1992.
10. Underwood, E.E. and Banerjee, K., In: *Metals Handbook*, Vol. 12. ASM International, Metals Park, Ohio, USA, 212-215, 1992.
11. Pook, L.P., *Crack Paths,* Wit Press, 2002.